World Academy of Science, Engineering and Technology
International Journal of Mechanical and Mechatronics Engineering
Vol:7, No:12, 2013

# Predictive Functional Control with Disturbance Observer for Tendon-Driven Balloon Actuator

Jun-ya Nagase, Toshiyuki Satoh, Norihiko Saga, Koichi Suzumori



***Abstract*—**In recent years, Japanese society has been aging, engendering a labor shortage of young workers. Robots are therefore expected to perform tasks such as rehabilitation, nursing elderly people, and day-to-day work support for elderly people. The pneumatic balloon actuator is a rubber artificial muscle developed for use in a robot hand in such environments. This actuator has a long stroke and a high power-to-weight ratio compared with the present pneumatic artificial muscle. Moreover, the dynamic characteristics of this actuator resemble those of human muscle. This study evaluated characteristics of force control of balloon actuator using a predictive functional control (PFC) system with disturbance observer. The predictive functional control is a model-based predictive control (MPC) scheme that predicts the future outputs of the actual plants over the prediction horizon and computes the control effort over the control horizon at every sampling instance. For this study, a 1-link finger system using a pneumatic balloon actuator is developed. Then experiments of PFC control with disturbance observer are performed. These experiments demonstrate the feasibility of its control of a pneumatic balloon actuator for a robot hand.

***Keywords*—**Disturbance observer, Pneumatic balloon, Predictive functional control, Rubber artificial muscle.

## I. Introduction

RECENTLY, because of progress of aging rapidly and the decrease of young workers in Japan [1], [2], robots are anticipated for use in nursing care and welfare services—performing rehabilitation and daily domestic tasks. Safety is a particularly important characteristic of robots for use in environments with humans. It necessitates dexterous, flexible movements similar to those of humans. Therefore, the impact force has decreased by making them lightweight; also, robots that use passive transformation elements have been developed [3]–[6].

Under such a circumstance, we have developed pneumatic tendon-driven balloon actuator (balloon actuator) [7] that has a long stroke and a high power ratio and is also compact and lightweight. Moreover the balloon actuator has been applied to the robot hand [8], [9].

The robot hand is required the force control of the finger in order to manipulate with dexterity an object and to grasping softly the soft object. However, in case of pneumatic rubber actuators including the balloon actuator, it is difficult to exact control because these actuators have non-linear property and change its characteristics.

In this study, the predictive functional control (PFC) [10], [11], that has high robustness and the parameter tuning is easy to achieve good control performance, is applied to the balloon actuator. PFC is one of Model predictive control (MPC); it has been developed for industry. Generally, calculated load of MPC is high because it demands to solve nonlinear optimization problem every sample time. Therefore the MPC is often applied to chemical plant that sample time is comparatively long. On the other hand, calculated load of the PFC is low because the control law consists of only the basis function. And, it is comparatively easy to tune the control parameter because the number of the parameter is only one. Moreover because PFC control system has internal model, it has high robustness for varying the property and the disturbance. In this paper, the PFC control performance with disturbance observer for the 1-link finger using the balloon actuator is evaluated.

## II. Predictive Functional Control

In this section we briefly overview the predictive functional control (PFC). Fig. 1 shows the basic concept of PFC. Suppose that the current time is labeled as time step $k$. A set-point trajectory is defined as a command signal which the process output $y_P$ should follow, and the value of the set-point trajectory at the current time step is denoted by $c(k)$. Also shown is a reference trajectory denoted by $y_R$. This trajectory starts at the current process output $y_P(k)$ and defines a desired trajectory along which the process output $y_P$ should approach the set-point trajectory. On the reference trajectory, there are a few coincidence points on which the performance index is defined and the process output $y_P$ should coincide with the reference trajectory $y_R$. As an example, three coincidence points are drawn in Fig. 3. The optimal control input trajectory is then computed on the basis of the predicted output.

Jun-ya Nagase is with Ryukoku University, Otsu, Shiga 520-2194 Japan (corresponding author to provide phone: +81-77-543-7434; fax: +81-77-543-7457; e-mail: nagase@rins.ryukoku.ac.jp).

Toshiyuki Satoh is with Akita Prefectural University, Yurihonjo, Akita 015-0055 Japan (e-mail: tsatoh@akita-pu.ac.jp).

Norihiko Saga is with Kwansei Gakuin University, Sanda, Hyogo 669-1337 Japan (e-mail: saga@kwansei.ac.jp).

Koichi Suzumori is with Okayama University, Okayama, Okayama 700-8530 Japan (e-mail: suzumori@act.sys.okayama-u.ac.jp).

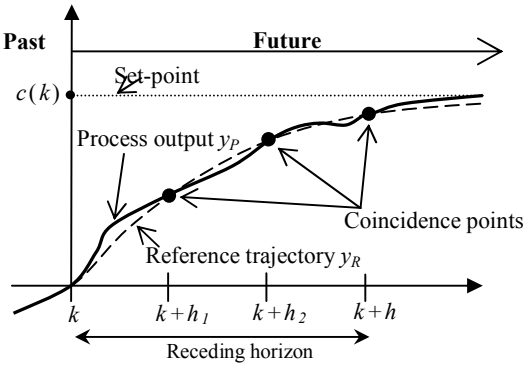


Fig. 1 Principle of predictive functional control

Once we have computed a future control input trajectory, we apply only the first element of the control input trajectory to the process. At the next time step, we repeat the whole cycle from the definition of the reference trajectory to the application of the first element of the optimal control input trajectory. We call this way of control a receding horizon control.

Next, we show the basic PFC algorithm using slightly modified formulation for handling time delay [12]. Now assume that the plant is stable and has the time delay of $L$ and that the sampling period is $T_s$. The development of PFC algorithm is based on the following SISO discrete-time linear state-space model of the plant:

$$x_M(k+1) = A_M x_M(k) + B_M u(k)$$

$$y_M(k) = C_M x_M(k) \tag{1}$$

where $x_M \in R^n$ is the state vector, $u \in R$ is the control input, $y_M \in R$ is the model output, respectively. Here, the model output $y_M(k)$ is used to predict the future plant output $y_P(k+d)$ where $d$ is defined as the nearest integer of $L/T_s$. Then the reference trajectory is defined as follows:

$$y_R(k+d+i) = c(k+d+i) - \alpha^i \left( c(k+d) - y_p(k+d) \right)$$

$$i = 0, 1, \ldots \tag{2}$$

where $\alpha \in R$ is a parameter which adjusts the approaching ratio of the reference trajectory to the set-point ($0<\alpha<1$). Empirically, the parameter $\alpha$has been chosen as $\alpha = e^{-3T_s}/T_{CLRT}$ along with the following three coincidence points

$$\begin{pmatrix} h_1 & h_2 & h_3 \end{pmatrix}^T = \begin{pmatrix} \frac{T_{CLRT}}{3T_s} & \frac{T_{CLRT}}{2T_s} & \frac{T_{CLRT}}{T_s} \end{pmatrix}^T \tag{3}$$

where $T_{CLRT}$ is called the desired closed-loop response time, which indicates the required time for the output response to arrive at 95% of the set-point. In PFC, $T_{CLRT}$ is the only design parameter, and we can balance the speed of response and the robustness by adjusting $T_{CLRT}$. In many cases, the performance index is defined as the quadratic sum of the errors between the predicted process output $y_P$ and the reference trajectory $y_R$ as follows:

$$D(k) = \sum_{j=1}^{n_h} \left\{ y_p(k+d+h_j) - y_R(k+d+h_j) \right\}^2 \tag{4}$$

where $h_j$ ($j$=0, 1, . . . , $h$) and $n_h$ are respectively the coincidence time point and the number of coincidence points. The minimization of the performance index (5) leads to the optimal control input as

$$u(k) = k_0 \left\{ c(k+d) - y_p(k) \right\} + \sum_{m=1}^{d_e} k_m c_m(k+d)$$

$$- \sum_{m=1}^{d_e} k_m e_m(k+d) + v_x^T x_M(k) + v_{xd}^T x_M(k-d) \tag{5}$$

where $d_e$ and $e_m$ are respectively the degree of the polynomial approximation and unknown coefficients that are computed on the basis of the past and present model error. Substances of $v_x$ and $v_{xd}$ are written in [13].

## III. 1-Link Finger Model with Balloon Actuator

### A. Pneumatic Tendon-Driven Balloon Actuator

The appearance and mechanisms of the pneumatic tendon-driven balloon actuator (balloon actuator) is portrayed respectively in Fig. 2. Table I shows the balloon specifications. Because the balloon actuator has high power-to-weight ratio and stroke-to-weight ratio, it can generate enough stroke and force for driving robot hand if it is installed in small space such a robot hand.

The balloon actuator is an air-pressure-drive type actuator comprising a silicone tube (balloon) and tendon wrapped around a tube. The silicone rubber tube is oval tube that the long diameter is 21mm, short diameter is 9mm and effective length is 9mm. The tube is sealed at one end to produce a balloon. Compressed air is supplied through an opening at the other end to expand the balloon. The tendon is made of polypropylene, and the nylon fiber sheet is stuck on one side of the tendon in order to decrease friction force generated between the tendon and the balloon. The tube is then fixed at both ends by acrylic plates. The wall is arranged on one side of the balloon to restrain its expansion. To decrease the loss of output efficiency, a roller is arranged in the part where the tendon direction is changed. A basic driving mechanism is as follows: The tendon wrapped around the balloon is expanded when the balloon expands, which creates tensile force for the tendon drive.

### B. 1-link Finger with Balloon Actuator

In this study, the control performance of the PFC of the balloon actuator is evaluated by conducting the control experiment of the 1-link finger system with the balloon actuator. Fig. 3 shows the photograph of 1-link finger system used in this study. This finger system is consists of the balloon actuator,

tension spring and finger. The finger flexes by restoration force of the tension spring and extends by tensile force of the balloon actuator. Therefore, when this finger system is implemented in a robot hand, this driving mechanism can prevent the fall of an object because the grip force can be secured by the spring if the system halts abnormally. The movable joint angle of the finger is 90 deg. almost same as human fingers'. The radius of the pulley is 11mm. The tension spring is the spring that the spring constant is 1.0 N/mm and initial force is 5.3N.

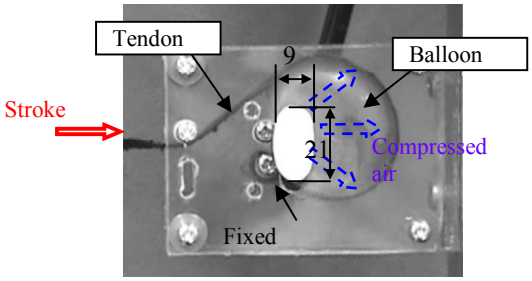


Fig. 2 Tendon driven balloon actuator

TABLE I
SPECIFICATION OF A BALLOON

| Material | Silicone rubber | |
|---|---|---|
| Length | 25 mm | |
| | Long diameter | Short diameter |
| Outer diameter | 21.0 mm | 9.0 mm |
| Inner diameter | 17.8 mm | 5.8 mm |

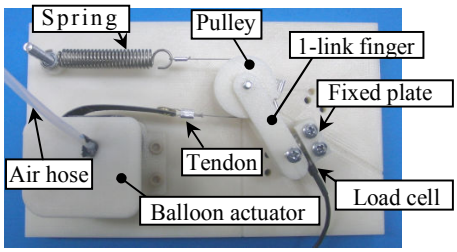


Fig. 3 Photograph of 1-link finger system using balloon actuator

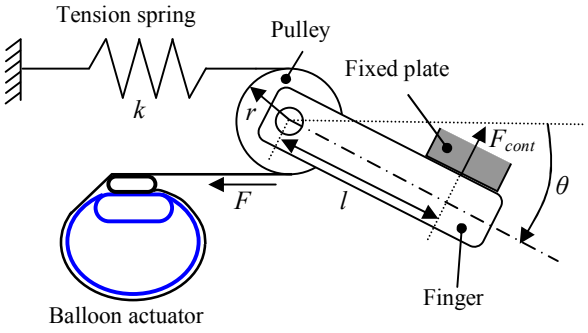


Fig. 4 1-link finger model using balloon actuator

Next, the physics model of the one-link finger can be described as follows. Fig. 4 shows a one-link finger model used for this study. To model the finger accurately, various parameters that affect response characteristics such as propagation velocity of compressed air, material nonlinear properties of a balloon, frictional force between the balloon and tendon, and viscoelasticity of a tendon, must be identified. However, it is extremely difficult to model them accurately by considering all of these parameters. In this study, because the purpose of the experiment is to conduct a comparative evaluation, the following simple mathematical model is used. The equation regarding with contact force $F_{cont}$ between finger and fixed plate is given as

$$rF_1(t) - lF_{cont}(t) = 0 \tag{6}$$

$$\dot{F}_1(t) + \alpha F_1(t) = \beta p_1(t) \tag{7}$$

where $r$ is the radius of the pulley, $l$ is the finger's length (30mm), viscous damping coefficient, and $\alpha$ and $\beta$ respectively represent unknown coefficients that depend on $p$.$F_1$ is given as

$$F_1(t) := F_0(t) - F(t) \tag{8}$$

$$p_1(t) := p_0(t) - p(t) \tag{9}$$

where $p$ is the internal pressure of the balloon, p0 is the internal pressure when $F_{cont}$ is zero, $F$ is the generated force of the balloon actuator, and $F_0$ is the generated force of the balloon actuator when $F_{cont}$ is zero. In this study, these model parameters are identified by experiments.

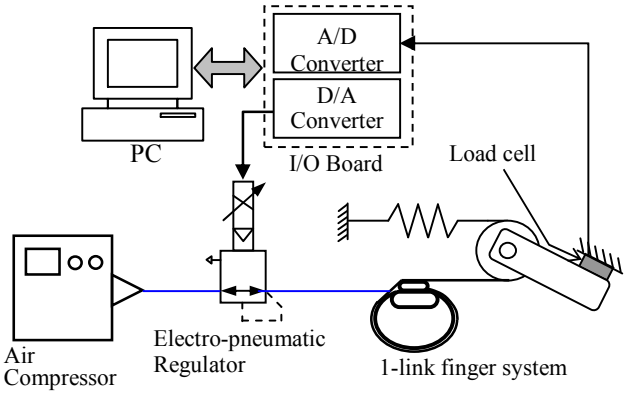


Fig. 5 Experimental system of force control of 1-link finger using balloon actuator

## IV. CONTROL EXPERIMENT

### A. Experimental Set-Up

Fig. 5 shows the experimental system used in this study. The compressed air to input to the balloon is provided from air-compressor [YC-4: Yaezakiku-atu Corp.]. The input air pressure is arranged using an electro-pneumatic regulator [ETR200-1; Koganei Corp.]. The joint angle of the finger is measured by potentiometer [SV03: Murata Manufacturing Co., Ltd.] installed in the finger joint. The measured angle is input to

the PC through the AD/DA board [Q4 PCI board : Quanser Corp.] with the sampling time set to 2 ms.

*B. Model Identification*

A PFC control system requires the internal model of the plant because it controls it using the predicted future plant output. Therefore, parameters of mathematical model described in the previous section are identified by an experiment. By (6) and (7), the transfer function from the applied internal pressure (MPa) to the contact force (N) can beapproximated by the following 1st order system.

$$G(s)=\frac{(l/r)(\beta/\alpha)}{s/\alpha+1} \tag{10}$$

Therein, $(l/r)(\beta/\alpha)$ and $1/\alpha$ represent gain and time constant respectively. In the experiment, after the step response characteristic of the finger contact force for the input pressure is measured, model parameters are identified by curve-fitting using the measured data. Because the discrete state space model such as (1) is necessary in the PFC control, the continuous transfer function model identified of (10) is discretized by Zero-Order Hold. It is transferred to the state space model.

*C. Disturbance Observer*

The prediction accuracy in the PFC scheme heavily depends on how precisely the model represents the real plant, so that the control performance of PFC could deteriorate when the real plant varies. Therefore, to compensate for the variation and nominalize the actual plant, we employ the disturbance observer [14]~[16], which is an effective disturbance compensation mechanism. The disturbance observer has the structure depicted in Fig. 6 where $P(s)$ is the transfer function of the real plant without time delay, $P_n(s)$ is the nominal model of the plant, $L$ is the time delay in the plant, and $Q(s)$ is a low-pass filter, which is also referred to as $Q$-filter. On the assumption that disturbances applied to the system and modeling errors can be regarded as an equivalent disturbance d at the plant input, the disturbance observer compares the actual delayed control input with its estimate obtained by multiplying the measured output y by the inverse nominal model $P_n(s)$-1 and computes the delayed estimate $d(t-L)$ of the current disturbance $d(t)$, which is subtracted from the controller output $u$ to cancel out the disturbance. As a result of this, we can impose the nominal input-output behavior on the real plant. The designed parameter of the disturbance observer is the filter $Q(s)$. To suppress the disturbance $d$, the gain of $Q(s)$ should be unity at low frequencies. On the other hand, to reject the measurement noise, the gain of $Q(s)$ should be0 at high frequencies. Therefore, $Q(s)$ must be a low-pass filter with the DC gain of 1. In this study, an analog Butterworth filter with 2 order is chosen as $Q(s)$ as shown following equation.

$$Q(s)=\frac{f^2}{s^2+1.414fs+f^2} \tag{11}$$

The cut-off frequency $f$ is decided to 60 Hz by experiment.

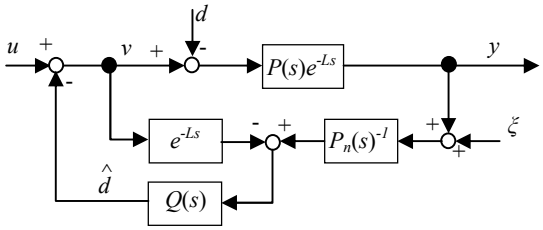


Fig. 6 Block diagram of disturbance observer

*D. Experimental Condition*

In the control experiment, the desired contact force of the finger is set to 1 N, 2N, and 3 N respectively. The control output for the step input is examined. Parameters of the PFC controller are $T_{CLRT}$, which is called the desired closed-loop response time as described above. The response speed increases when $T_{CLRT}$ is decreased because it indicates the desired closed-loop response time. However, in that case, the robust stability decreases because it is affected easily by noise of the plant output and modeling error. In this study, the smallest $T_{CLRT}$ is chosen such that it does not become a vibrational response. It is set to 0.10 s.

*E. Experimental Results*

First, control performances for step input are discussed. Fig. 7 presents experimentally obtained results for PFC and PFC with disturbance observer. The black solid line represents the desired value. The blue dashed line and the red solid line represent results of PFC and PFC with disturbance observer respectively. Regarding comparison of the transient characteristics, the settling time of PFC is about 1.0 s on each desired force. On the other hand, that of PFC with disturbance observer is about 0.7 s respectively. Fig. 8 shows the responses of the predicted output and the actual plant output. We can see from Fig. 8 that, without the disturbance observer, the predicted output considerably differs from the plant output. On the other hand, the predicted output promptly coincides with the actual plant output when we use the disturbance observer. These indicate that the PFC control performance is improved by using disturbance observer because the accuracy of the predicted output is increased.

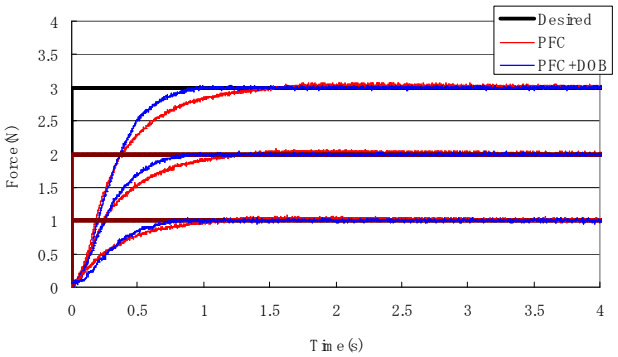


Fig. 7 Experimental result of force control for step input

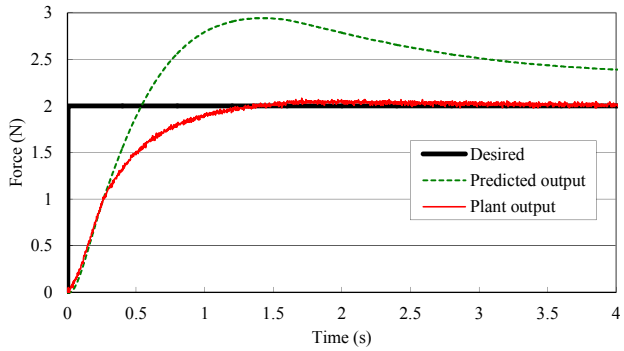


(a) Without disturbance observer

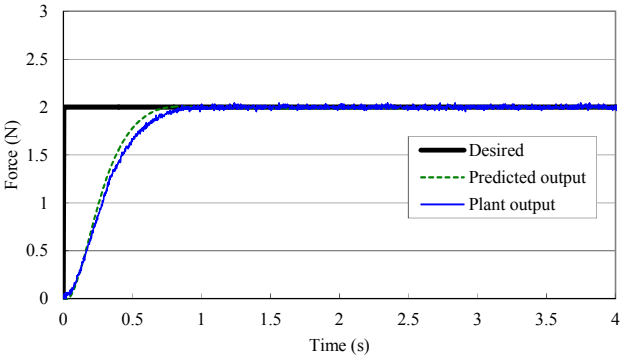


(b) With disturbance observer

Fig. 8 Comparison of predicted accuracy with or without disturbance observer

Fig. 9 (a) shows the experimental result of force control to sinusoidal input. The black solid line represents the desired value. The blue dashed line and the red solid line represent results of PFC and PFC with disturbance observer respectively. As a result, the controlled variable of PFC is delayed for the desired variable greatly. On the other hand, the controlled variable of PFC with disturbance observer tracks well for the desired variable. Fig. 9 (b) shows the error force of controlled variable for the desired variable. The maximum errors of PFC and PFC and PFC with disturbance observer are 0.23 N and 0.13N respectively. These results indicate that the disturbance observer improves the tracking performance of the contact force of balloon actuator in PFC control system.

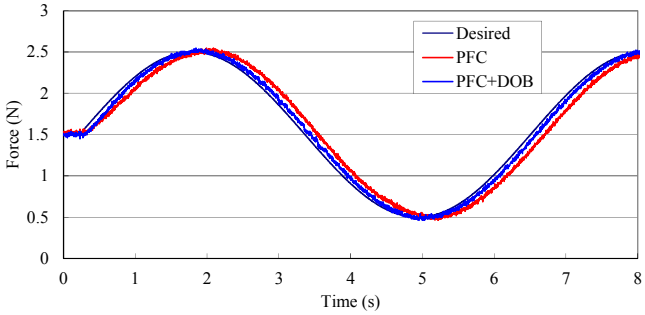


(a) Plant output

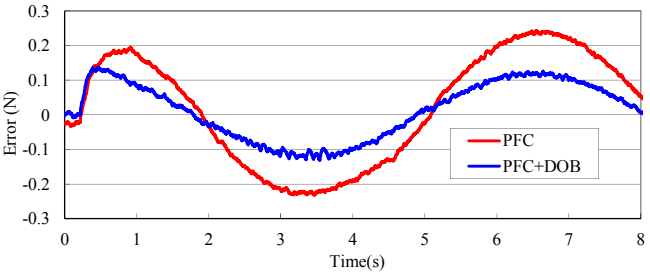


(b) Tracking error

Fig. 9 Experimental result of force control for sinusoidal input

## V. Conclusions

In this study, force control characteristics of the balloon actuator by PFC control using 1-link finger system are evaluated. Our conclusion is as follows:

In the experiment of the force control for the step input, in case of PFC control, the predicted output of the contact force does not converge in the desired value of that. However, by applying the disturbance observer, the predicted output promptly coincides with the actual plant output. In consequence, the PFC control performance has improved about 30% by using disturbance observer. In the experiment of force control to sinusoidal input, the disturbance observer improves the tracking performance of the contact force of the balloon actuator more than 40%.

## Acknowledgment

This research was supported by a "Grant-in-Aid for Young Scientists (B) (No. 23760246)".

## References

[1] http://www.hei.co.jp/Products/e_m_g/ph_sh_2.html
[2] http://www.ipss.go.jp/ppnewest/j/newest03/newest03.asp
[3] K. Suzumori, S. Iikura, H. Tanaka, "Applying a Flexible Microactuator to Robotic Mechanisms", *IEEE Control Systems*, Vol.12, No.1, pp.21-27, 1992.
[4] T. Noritsugu, M. Kubota, S. Yoshimatsu, "Development of Pneumatic Rotary Soft Actuator Made of Silicone Rubber", *Journal of Robotics and Mechatronics*, Vol.13, No.1, pp.17-22, 2001.
[5] http://www.shadow.org.uk/products/newhand.shtml
[6] http://www.festo.com/cms/en-gb_gb/5001.htm
[7] J. Nagase, N. Saga, "Two Tendon Driven Systems Using Pneumatic Balloons", *Advanced Robotics*, Vol. 25, No. 9-10, pp.1349-1361, 2011.
[8] J. Nagase, N. Saga, T. Satoh, and K. Suzumori, "Development and Control of a Multi-Fingered Robotic Hand Using a Pneumatic Tendon-driven Actuator", *Journal of Intelligent Material Systems and Structures*, Vol.23, No.3, pp.339-346, 2012.

[9] J. Nagase, S. Wakimoto, T. Satoh, N. Saga, and K. Suzumori, "Design of variable-stiffness robotic hand using pneumatic soft rubber actuators", *Smart Materials and Structures*, Vol.20, No.10, 105015(pp.1-9), doi:10.1088/0964-1726/20/10/105015, 2011

[10] J. Richalet, S. Abu el Ata-Doss, C. Arber, H.B. Kuntze, A. Jacubasch, W. Schill, "Predictive functional control: application to fast and accurate robot", *Proc. of IFAC 10th World Congress*, pp.251-259, 1987.

[11] J. Richalet, "Industrial applications of model based predictive control", *Automatica*, Vol.29, No.5, pp.1251-1274, 1993.

[12] T. Satoh, N. Saito, N. Saga, "Predictive functional control with disturbance observer for pneumatic artificial muscle actuator", *Proc. of the 1st International Conference on Applied Bionics and Biomechanics*, 2010.

[13] J. Y. Dieulot, T, Benhammi, F. Colas, P.J. Barre, "Composite predictive functional control strategies", Application to positioning axes, *International Journal of Computers, Communications & Control*, Vol. III, No.1, pp.41-50, 2008.

[14] K. Ohishi, M. Nakao, K. Ohnishi and K. Miyachi, "Microprocessor controlled DC motor for load-insensitive position servosystem," *IEEE Trans. on Industrial Electronics*, vol. 34, no. 1, pp.44-49, 1987.

[15] T. Murakami and K. Ohnishi, "Advanced motion control in mechatronics– A tutorial," *Proc. of the IEEE International Workshop on Intelligent Control*, Istanbul, Turkey, vol. 1, pp. SL9-SL17, 1990.

[16] T. Umeno and Y. Hori, "Robust speed control of DC servomoters using modern two-degrees-of-freedom controller design," *IEEE Trans. on Industrial Electronics*, vol. 38, no. 5, pp. 363-368, 1991.